Supporting information

Stable Cascade Dual Z-Scheme SnC/Arsenene/HfS2 Trilayer Heterojunction for High-Efficiency Photocatalytic Water Splitting: A First-Principles Study

Zhengdong Sun[a], Jiaxin Ma[a], Junhao Zhu[a], Yifei Shen[a], Zhuyuan Shen[a], Yiqing Liu[a], Weide Liu[a], Minwei Zhang[a], Meng Zhang*[a]

[a] School of Physics, East China University of Science and Technology, Shanghai 200237.

* Corresponding author: E-mail: mzhang@ecust.edu.cn (M. Zhang)

1. Structural Parameters of Different Stacking Configurations for Two Trilayer Heterojunctions

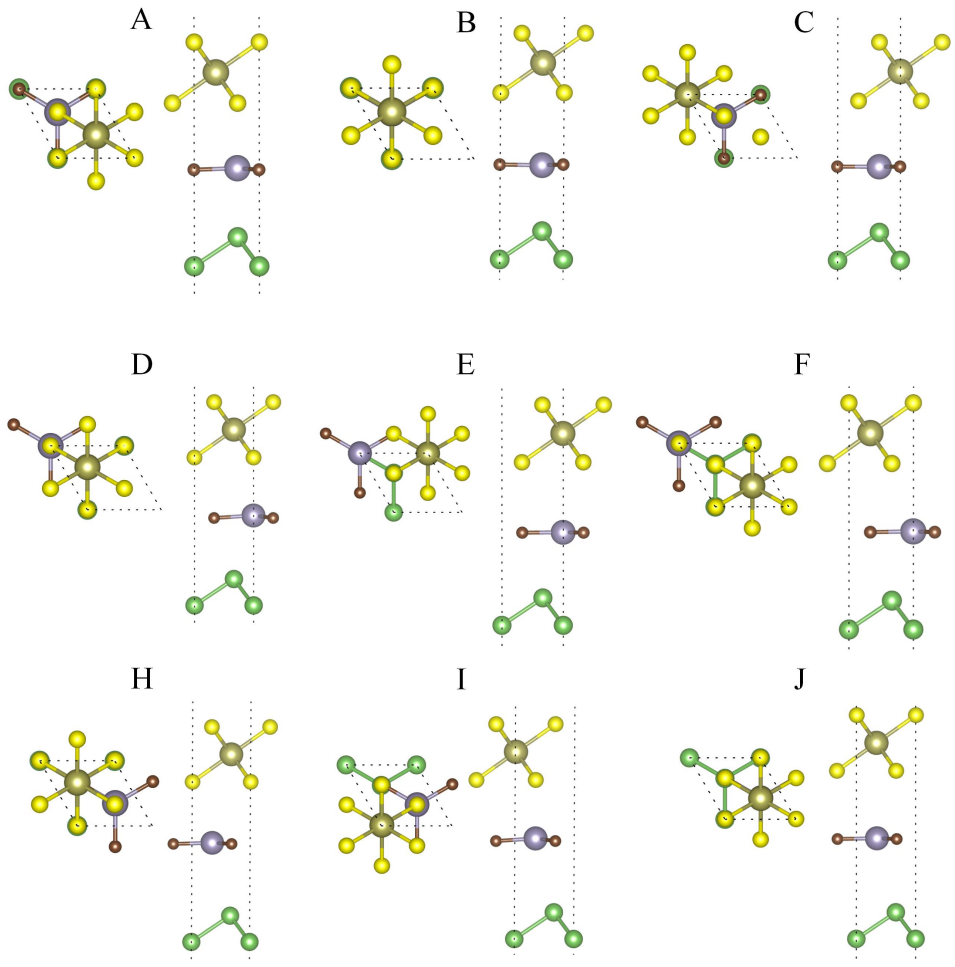

Fig. S1. Top and side views of the nine stacking configurations for the HfS_2/SnC/arsenene heterojunction. Each configuration corresponds to a distinct relative lateral displacement among the three monolayers.

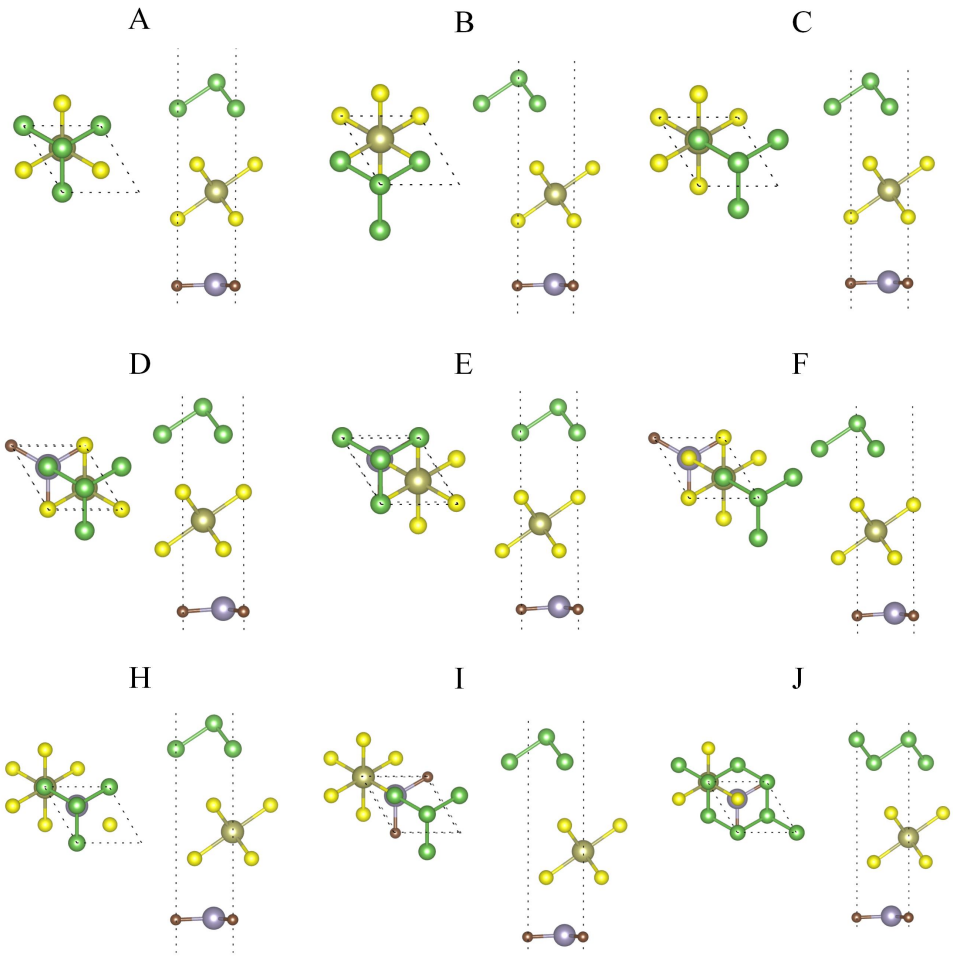

Fig. S2. Top and side views of the nine stacking configurations for the arsenene/HfS_2/SnC heterojunction.

Table S1. Calculated lattice constants, interlayer spacings, and binding energies of the HfS_2/SnC/arsenene heterojunction in different stacking configurations. Notes: $d_{HfS2\text{-}SnC}$ and $d_{SnC\text{-}arsenen}$ represent the interlayer distances between adjacent monolayers.

Configurations	Lattice (Å)	$d_{HfS2\text{-}SnC}$(Å)	$d_{SnC\text{-}arsenene}$(Å)	E_b(eV)
A	3.606	3.119	3.308	-1.170
B	3.605	3.569	3.242	-1.084
C	3.606	3.276	3.271	-1.138
D	3.603	3.067	3.360	-1.154
E	3.602	3.557	3.338	-1.058
F	3.603	3.275	3.344	-1.116
H	3.598	3.248	3.889	-1.039
I	3.598	3.073	3.877	-1.079
J	3.597	3.556	3.896	-0.980

Table S2. Calculated lattice constants, interlayer spacings, and binding energies of the arsenene/HfS_2/SnC heterojunction in different stacking configurations.

Configurations	lattice (Å)	$d_{arsenene-HfS2}$(Å)	$d_{HfS2-SnC}$(Å)	E_b(eV)
A	3.597	3.001	3.532	-1.063
B	3.595	3.581	3.542	-0.983
C	3.597	3.103	3.555	-1.048
D	3.598	2.965	3.060	-1.163
E	3.596	3.557	3.086	-1.084
F	3.598	3.092	3.086	-1.147
H	3.598	3.081	3.268	-1.107
I	3.597	3.575	3.238	-1.043
J	3.598	3.007	3.240	-1.123

2. Stability Analysis of Trilayer Heterojunctions

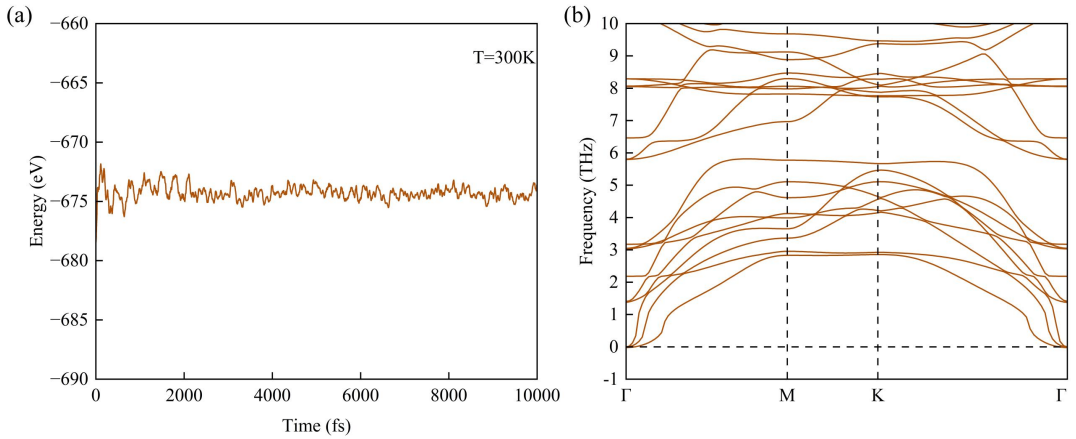

Fig. S3. (a) Total potential energy evolution of the HfS_2/SnC/arsenene heterojunction during ab initio molecular dynamics (AIMD) simulation at 300 K over 10 ps. (b) Phonon dispersion spectrum confirming dynamic stability of the same configuration.

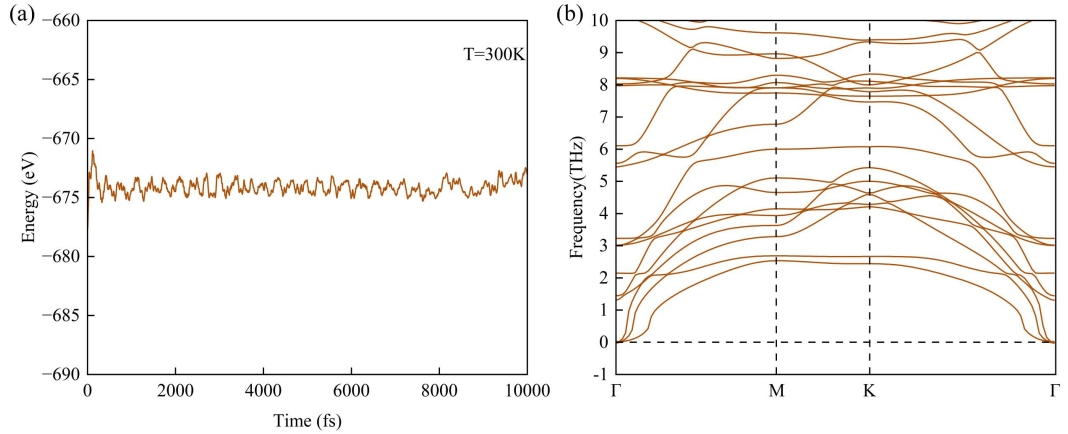

Fig. S4.(a) AIMD simulation showing the total energy variation of the arsenene/HfS_2/SnC heterojunction at 300 K. (b) Corresponding phonon spectrum confirming dynamic stability without imaginary frequencies.

3. Adsorption Configurations of HER and OER Intermediates

To eliminate spurious periodic interactions, 4×4 supercells were constructed for the three heterojunctions, and adsorption configurations for key intermediates in the hydrogen and oxygen evolution reactions were simulated.

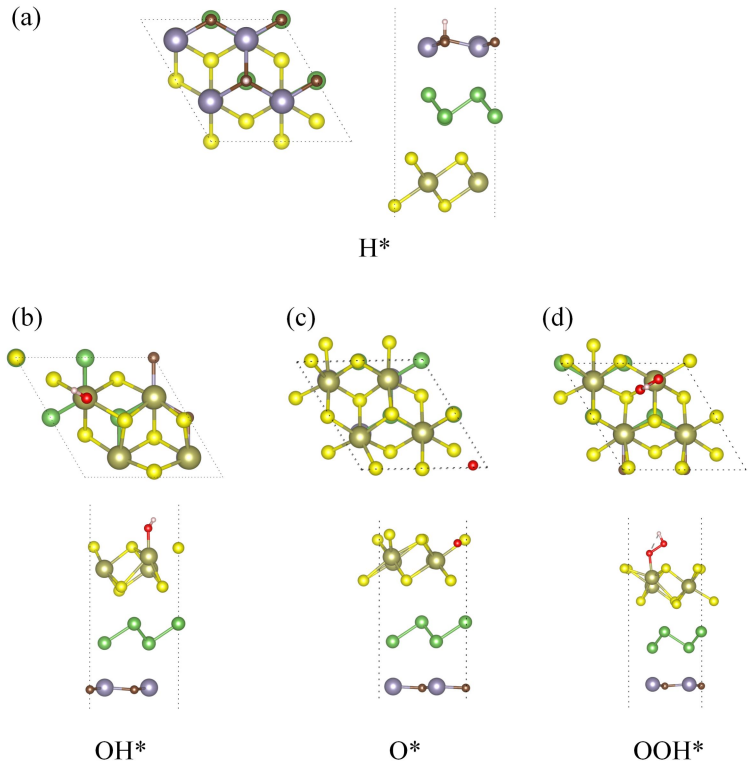

Fig. S5. Adsorbed intermediate configurations in the cascade dual Z-scheme SnC/arsenene/HfS_2 heterojunction: (a) hydrogen evolution reaction (HER); (b) oxygen evolution reaction (OER).

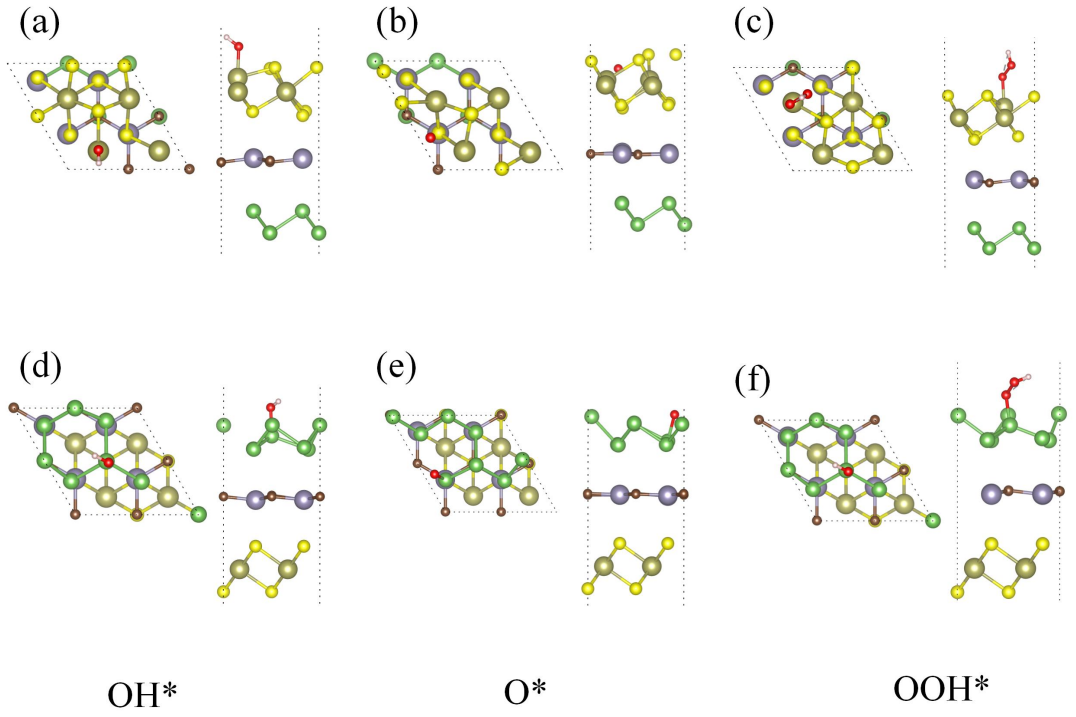

Fig. S6. OER intermediate adsorption configurations for the arrow-up dual Z-scheme HfS_2/SnC/arsenene heterojunction: (a–c) adsorption on the HfS_2 side; (d–f) adsorption on the arsenene side.

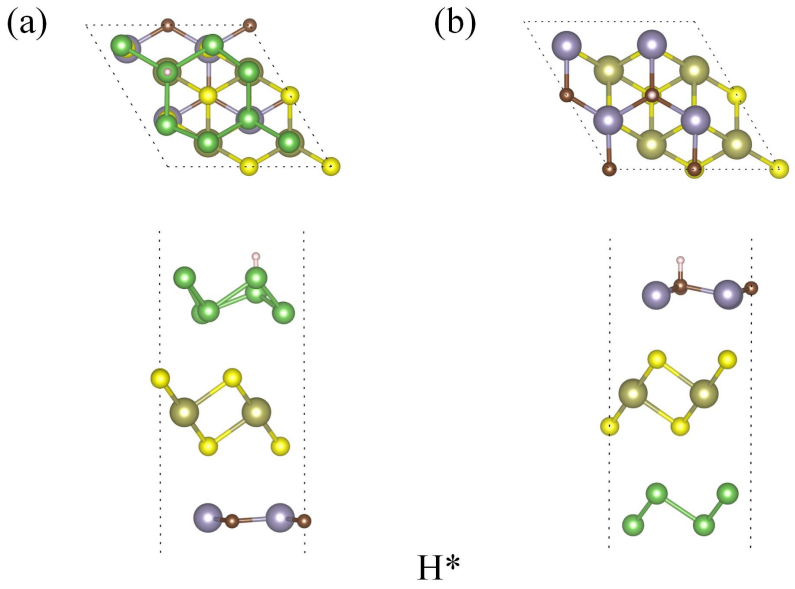

Fig. S7.HER intermediate adsorption configurations in the arrow-down dual Z-scheme arsenene/HfS_2/SnC heterojunction: (a) arsenene side; (b) SnC side.

4. Gibbs free energy step diagram for HER and OER

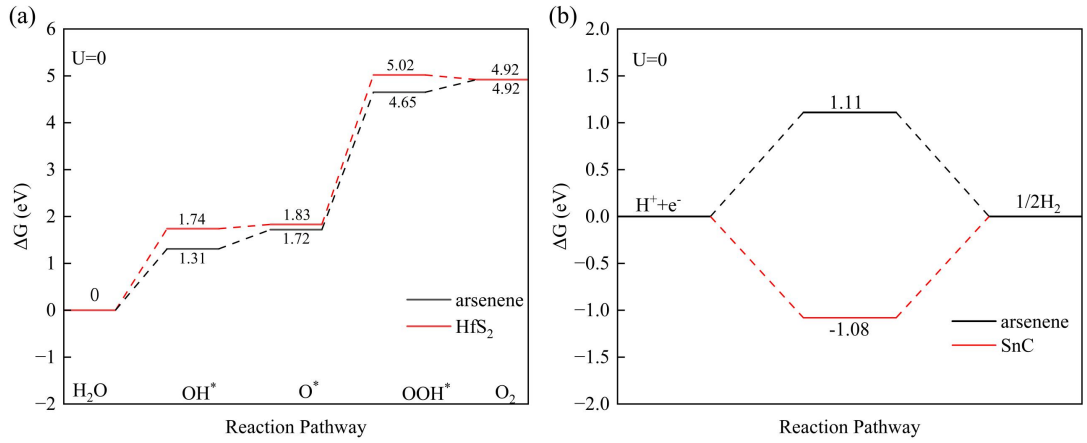

Fig. S8. The Gibbs free energy steps of (a) the reduction reaction on the arsenene side and HfS_2 side and (b) the oxidation reaction on the arsenene side and SnC side in arrow-up dual Z-scheme HfS_2/SnC/arsenene heterojunction and arrow-down dual Z-scheme SnC/arsenene/HfS_2 heterojunction, respectively.

5. Optical Properties of Trilayer Heterojunctions

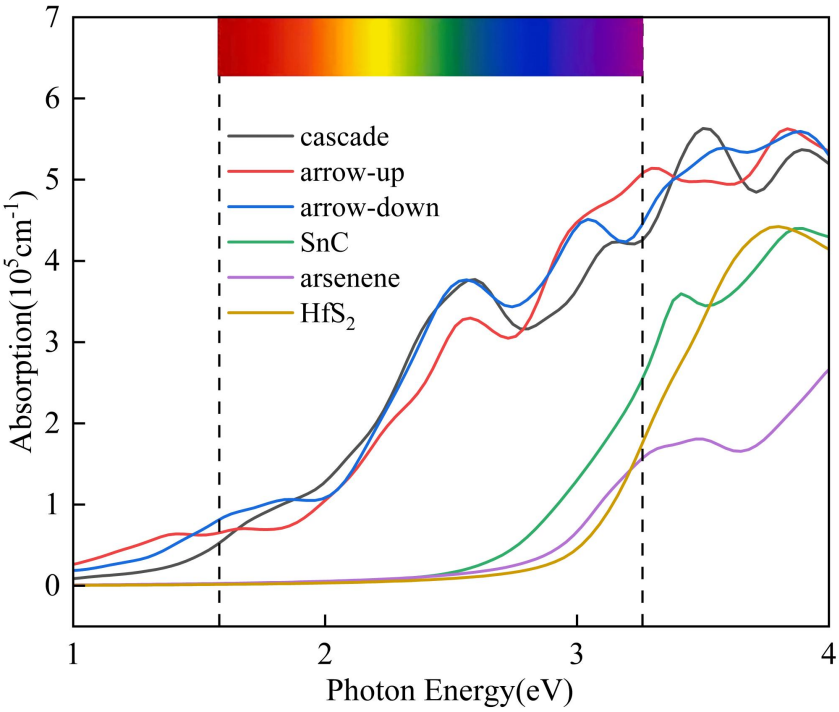

Fig. S9. Optical absorption spectra of monolayer SnC, arsenene, and HfS_2, as well as the cascade, arrow-up, and arrow-down SnC/arsenene/HfS_2 trilayer heterojunctions studied in this work.